



# Zircon SHRIMP U-Pb Dating and Significance From Weathered Residual Kaolin Deposits on the Northern Margin of the Qinzhou-Hangzhou Suture Zone, China

Chunhai Li<sup>1,2,3\*</sup>, Qifa Sun<sup>1</sup>, Zhonglin Sun<sup>1</sup>, Xiaohua Zhou<sup>2</sup>, Wei Zhang<sup>2</sup>, Rong Chen<sup>2</sup> and Tianshan Gao<sup>2</sup>

## OPEN ACCESS

### Edited by:

Lidong Dai,  
Institute of geochemistry (CAS), China

### Reviewed by:

Mingliang Wang,  
Suzhou University, China  
Lv Zheng-Hang,  
Institute of Geochemistry (CAS), China

### \*Correspondence:

Chunhai Li  
lichunhai01@sina.com.cn

### Specialty section:

This article was submitted to  
Geochemistry,  
a section of the journal  
Frontiers in Earth Science

**Received:** 15 January 2022

**Accepted:** 07 February 2022

**Published:** 31 March 2022

### Citation:

Li C, Sun Q, Sun Z, Zhou X, Zhang W,  
Chen R and Gao T (2022) Zircon  
SHRIMP U-Pb Dating and Significance  
From Weathered Residual Kaolin  
Deposits on the Northern Margin of the  
Qinzhou-Hangzhou Suture  
Zone, China.  
Front. Earth Sci. 10:855459.  
doi: 10.3389/feart.2022.855459

<sup>1</sup>Harbin Natural Resources Comprehensive Investigation Center, China Geological Survey, Harbin, China, <sup>2</sup>Nanjing Geological Survey Center, China Geological Survey, Nanjing, China, <sup>3</sup>School of Earth Science and Engineering, Nanjing University, Nanjing, China

Weathered residual Kaolin deposits on the northern margin of the Qinzhou-Hangzhou Suture Zone are characterized by more feldspar-containing minerals and fewer dark minerals. These deposits have attracted increasing attention because of their high whiteness, low harmful impurity content, low depth of weathered mineralization, and ease for mining. The ore-forming rock masses mainly include granite (granite porphyry), quartz porphyry, eurite, haplite, and other acidic veins; the ore-bearing walls are mainly of Upper Proterozoic. Previous studies suggested that dyke rocks related to Kaolin deposits in this belt belong to the Mesozoic, but there is a lack of information regarding specific mineralization ages. In this study, two dyke wall-type weathered residual Kaolin deposits were selected from the northern margin of the Qinzhou-Hangzhou Suture Zone (Dongxicun and Yinbeidong, Jiangxi Province, China) for zircon SHRIMP dating. Two zircon U-Pb-based ages were obtained:  $843 \pm 10$  Ma from Dongxicun granite veins that intrude into the Neoproterozoic Jiuling rock masses;  $152.3 \pm 1.8$  Ma for Yinbeidong granite porphyry veins that intrude into the Neoproterozoic Anlelin Formation. We suggest that the dykes related to the Kaolin deposits were formed in the Neoproterozoic and late Jurassic. The Neoproterozoic dyke may be related to the convergence, formation, or pyrolysis of the Rodinia Supercontinent and the late Jurassic dyke may be related to the subduction of the Paleo-Pacific Plate. These results provide a chronological basis for the investigation and evaluation of weathered residual Kaolin deposits on the Qinzhou-Hangzhou Suture Zone.

**Keywords:** kaolin deposit, zircon U-Pb dating, weathered eluvial deposit, Jiangxi province, Qinzhou-Hangzhou suture zone

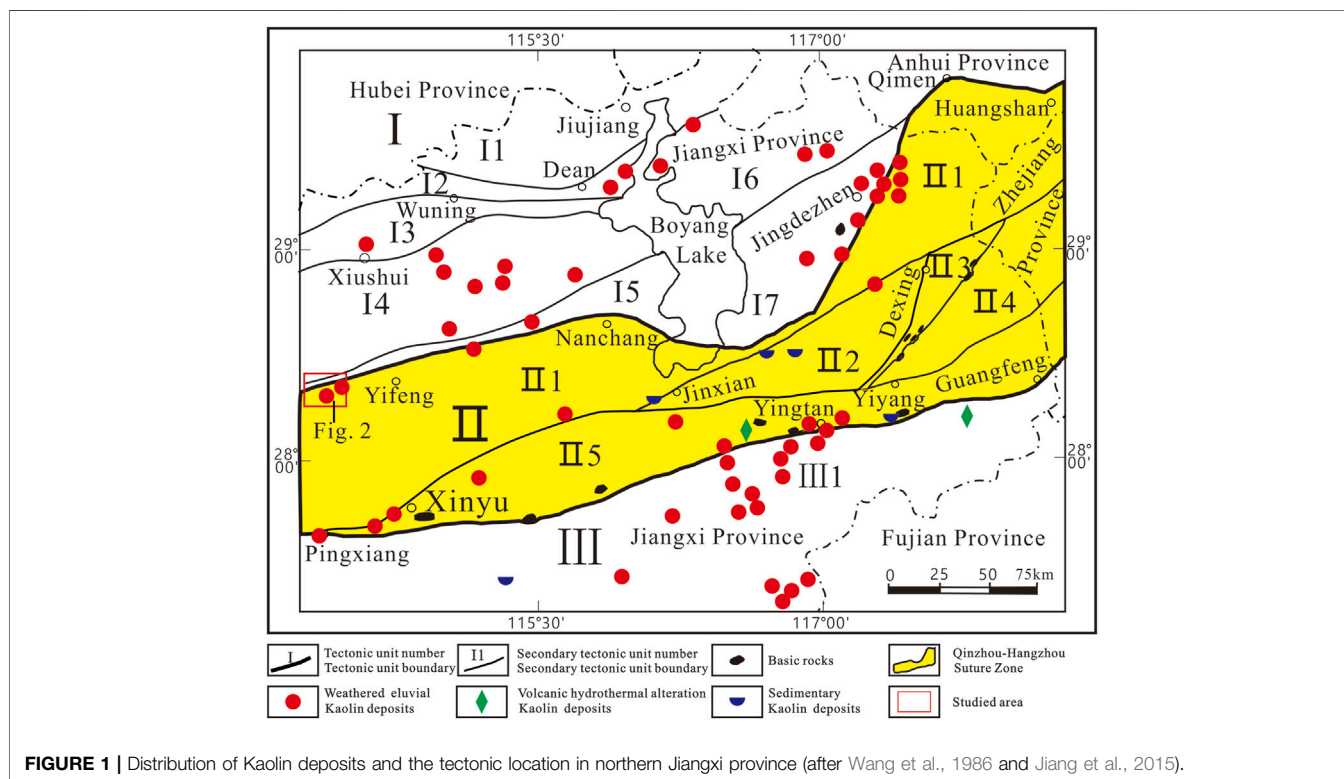
## INTRODUCTION

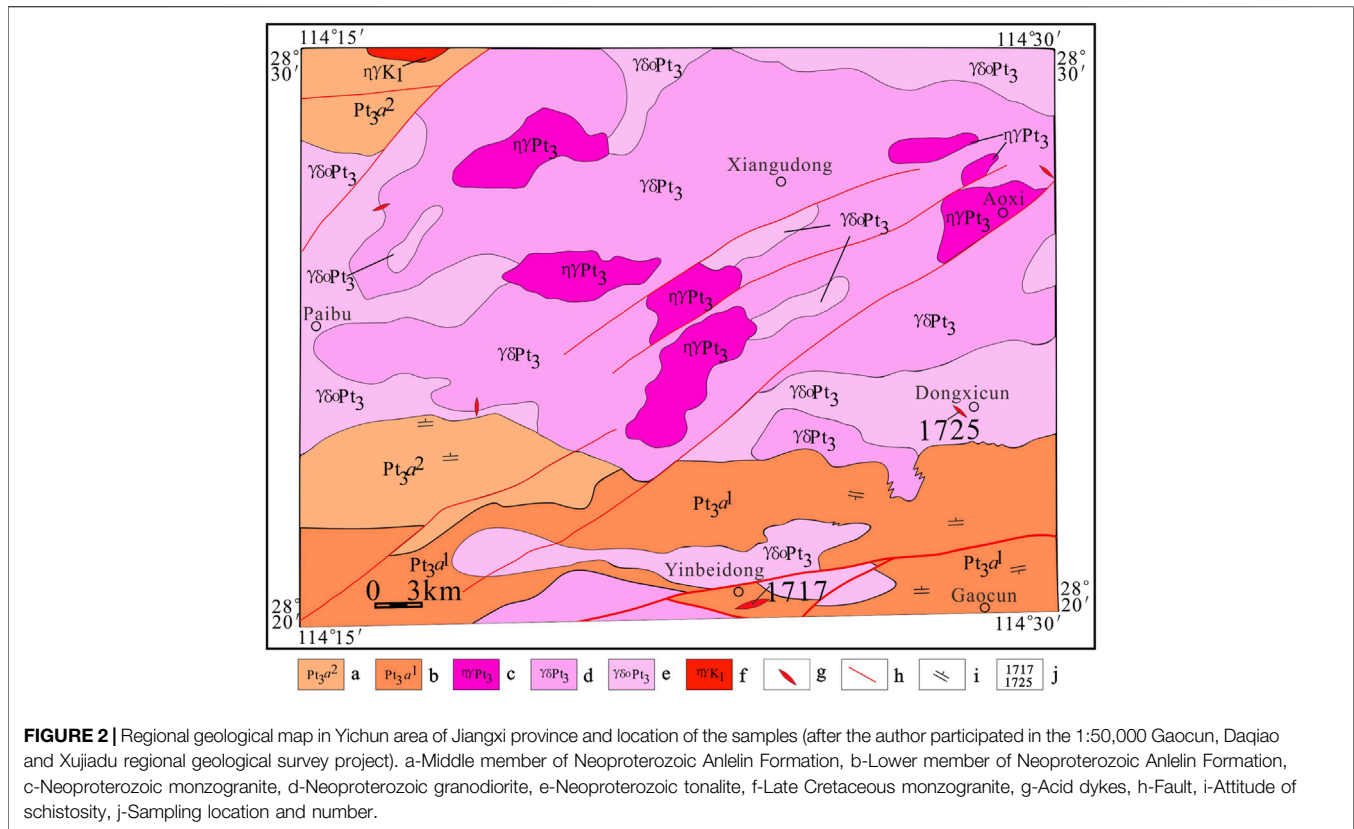
The northern Jiangxi Province is geologically complex with frequent magmatic activity in the Proterozoic and Mesozoic. This region has relatively rich Kaolin resources and ranks among the top in China in terms of reserves. There are nearly 100 known Kaolin deposits and ore sites (Figure 1), among which the most representative is in the village of Gaoling (Ehu, Fuliang County) in northeastern Jiangxi (Li et al., 2017; Wang et al., 2018). The Kaolin deposits are divided into three types: weathered residual; volcanic hydrothermal alteration; sedimentary. Weathered residual Kaolin deposits are very important in terms of reserves and mining quantities. Their formation is mainly affected by the ore-forming parent rock masses, tectonic conditions, and water conditions; ore-forming parent rock masses mainly include granite, pegmatite, and other acidic veins.

I-Yangtze Plate, I1-Low Yangtze Tectonic Unit, I2-Jiugong Mountain Tectonic Unit, I3-Wuning-Xiushui Tectonic Unit, I4-Jiuling Mountain Tectonic Unit, I5-South Edge of Jiuling Mountain Tectonic Unit, I6-Zhanggong Mountain Tectonic Unit, I7-Leping Tectonic Unit, II-Qingzhou-Hangzhou Suture Zone, II1- Leping-Shexian Melange Subzone, II2-Wannian Tectonic Unit, II3-Ophiolite Melange Subzone of Northeast Jiangxi, II4-Huaiyu Mountain Tectonic Unit, II5-Dongxiang-Longyou Ophiolite Melange Subzone, III-Cathaysia Plate, III1-Wugong Mountain- North WuYi Mountain Tectonic Unit.

Yichun is located in northwestern Jiangxi Province, with its geotectonic position on the northern margin of the Qinzhou-Hangzhou Suture Zone (QHSZ) or the Qinzhou-Hangzhou

Metallogenic Belt (QHMB) between the Yangtze and Cathaysia plates (Figure 1), roughly equivalent to the Jiangnan Orogenic Belt. The known mineral resources mainly include copper, gold, tungsten, iron, coal, lithium, niobium-tantalum, Kaolin, cement, and groundwater. Among these, Kaolin deposits have attracted more and more attention due to their high whiteness, low content of harmful impurities, and ease of mining. The weathered residual Kaolin deposits in Yichun (Jiangxi Province) were formed through superficial weathering of aluminum-rich silicate. Hydrothermal alterations such as illitization and Kaolinization frequently occur, so Kaolin deposits are easily weathered. Acidic veins these form Kaolin deposits from weathered residualization are also controlled by regional faults and characterized by a zonal distribution. In general, the acidic veins include more feldspar-containing minerals, mainly Kaolinite, illite, feldspar, and sericite, but fewer dark minerals, such as biotite and hornblende. The minerals are rich in  $Al_2O_3$  (more than 15%) and have a low content of harmful impurities, such as  $TiO_2$  and  $Fe_2O_3$  (more than 3% in total). Despite their small scale, the deposits are found in large quantities and at low weathered mineralization depths, and are often produced in groups and belts ranging from tens to hundreds of meters in length. A single vein has a width of one to 6 m and a single vein belt has a width of tens of meters, which makes the deposits mining targets. The ore-forming rock masses mainly include granite, granite porphyry, quartz porphyry, eurite, haplite, and other veins, and the intrusive wall rocks are mainly of Neoproterozoic age. Wang and Fang (1994) conducted a preliminary study of the characteristics and formation mechanisms of high-quality Kaolin deposits in Yichun using





microscopic identification and chemical composition analysis. They found that the Kaolin is mainly composed of Kaolinite minerals (largely scaly Kaolinite and tubular 7 A halloysite), lepidolite (white mica), albite, quartz, and potash feldspar. Heavy minerals include apatite, topaz, microlite, and niobium-tantalite, but almost no iron oxide minerals, which may be related to the post-magmatic hydrothermal alteration of albite. These regional data suggested that most of the acidic veins that form Kaolin deposits occurred during the Mesozoic, but there is a lack of data for specific mineralization ages. In this study, we selected two weathered residual Kaolin deposits from Dongxicun and Yinbeidong in Yichun (northern QHMB margin) for zircon SHRIMP U-Pb dating and recorded two ages from veins in Kaolin deposits,  $843 \pm 10$  Ma (granite veins in deposits intruding into Jiuling tonalite masses) and  $152.3 \pm 1.8$  Ma (granite porphyry veins in deposits intruding into the Anlelin Formation). These two specific U-Pb ages could reveal a chronological basis for the investigation and evaluation of weathered residual Kaolin deposits on the Qinzhou-Hangzhou Suture Zone.

## GEOLOGICAL BACKGROUND

In the region, Upper Proterozoic and Quaternary strata are distributed over a large area (Figure 2), and the Carboniferous–Triassic, Jurassic, and Cretaceous Systems are sporadically exposed. The Proterozoic Erathem in the region is

mainly composed of the Yifeng Formation Complex and the Anlelin Formation. Lithologically, the Yifeng Formation is mainly sericite (quartz) phyllite (partly schist) containing inter-layers (or lens) of metatuffaceous rocks, silty sand, and metaplasia-horn porphyry (metadiabase). The Carboniferous–Triassic System is mainly composed of carbonate deposits, with lesser deposits of mudstone. The Jurassic System is mainly composed of carbonate–clastic deposits. The Cretaceous System is mainly composed of red, mostly coarse, clastic rocks. The rock masses are mainly from the Neoproterozoic Jiuling terrane and the Mesozoic rock masses are mostly present in the form of rock strains or veins.

The QHSZ has undergone multiple periods of tectonic deformation. The tectonic traces are mainly NE-trending folds–faults and a NW-trending fault zone, followed by a near EW-trending fault zone. The near EW-trending tectonic zone formed earlier than the NW-trending fault zone and both are mostly filled by veins. The NE-trending fault zone was the latest formed (or had the longest active period), and features large scale and multiple periods. The exposed Anlelin Formation is mainly of Proterozoic age. The lower section is a thickly layered variable residual fine to medium-grained lithic sandstone intercalated with silty slate. The middle section is thin–medium layered variable residual siltstone and silty slate, containing variable residual fine-grained lithic sandstone and metastatic tuff inter-layers (or lens). The Neoproterozoic Jiuling compound rock masses are mainly exposed and are produced in the form of rock bases. Lithologically, from old to new, they are roughly

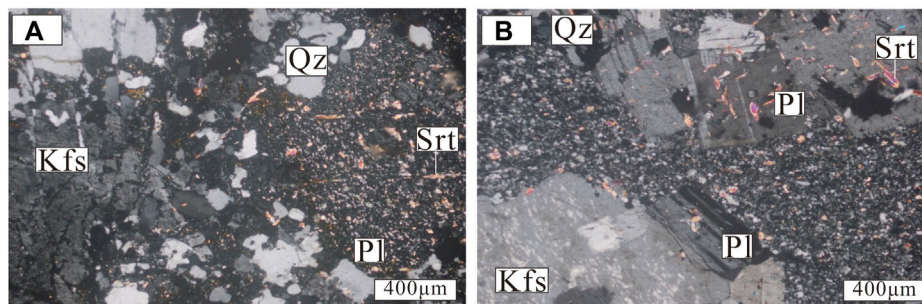


**FIGURE 3** | Photomicrographs of the granite dyke (Sample 1725) **(A)** and the granitic porphyry dyke (Sample 1717) **(B)** Qz-quartz; Pl-plagioclase; Kfs-potash feldspar; Srt-sericite.

tonalite, granodiorite, and monzogranite. Previously reported ages of the Jiuling rock masses are mainly derived from samples on the northern margin and are generally 816 to 837 Ma (Zhong et al., 2005; Yuan et al., 2012; Duan et al., 2019). The Mesozoic rock masses have a small exposed area and are predominantly present in the form of rock strains and veins. They are mainly granites with some Kaolin deposits weathered from granite veins.

## SAMPLING

Samples for this study were recovered from the newly mined village of Dongxicun and Yinbeidong Kaolin deposits in Yichun (Figure 2). The ore-forming granite vein (Sample 1725) of the Kaolin deposits in Dongxicun is distributed along the NW and intrudes into the Neoproterozoic Jiuling medium to fine-grained tonalite masses. The exposed width of the vein zone is 10–20 m, the current mining depth is over 6 m. Granite veins, which became yellow–white and fine to medium-grained structures upon weathering, are mainly composed of feldspar and quartz. The feldspars are yellowish-white, white, and earthy upon weathering, and mainly include plagioclase feldspar (35% abundance; 0.5–1.5 mm), mostly sericitized potassium feldspar (20%; 0.7–2.0 mm), and colorless quartz (35%; 0.3–1.5 mm) that features hypautomorphic-allotriomorphic filling (Figure 3A). Biotite has been altered by chlorite and limonite, with a content of less than 3%. Accessory minerals include trace amounts of apatite and magnetite.

Distributed in a near EW direction, the Yinbeidong Kaolin ore-forming granite porphyry vein (Sample 1717) roughly occurs at  $345^\circ < 88^\circ$  and intrudes into the plate-like metasiltstone of the Neoproterozoic Anlelin Formation. The exposed width of the vein is about 20 m, the current mining depth is over 4 m. Quartz veinlets have developed in veins and plate-like metasiltstones. The veinlet density is 8–10 pieces/m, with single pieces 0.6–4 cm in width; the occurrence of the veinlets is similar to the granite porphyry intrusion surfaces. After weathering, the granite porphyry vein is white (slightly greenish-white when fresh) with a porphyritic structure. Phenocrysts (about 30%) are mainly feldspar and the matrix (about 70%) is mainly felsic rock and biotite (< 0.5%) with a rust-colored surface upon

iron precipitation and weathering. Feldspar phenocrysts are mainly plagioclase feldspar, with polysynthetic twins and Carlsbad-albite compound twins. The surface is mostly sericitized, white and subhedral (1.5–2.5 mm). The potassium feldspar phenocrysts (1.5–3.0 mm) have a striped structure and are allotriomorphic. Quartz (0.3–1.5 mm) is allotriomorphic and mostly filled with other mineral particles, with obvious wavy extinction (Figure 3B). Local chloritization and ferritization occurs, with few iron mineral particles. The accessory minerals include trace amounts of apatite and magnetite. Plate-like metasiltstone xenoliths of the Anlelin Formation are present in the veins, with sulfide aggregates such as pyrite and marcasite occasionally observed. Pyrite (0.5–2 mm) is light yellow and cube-shaped, while marcasite (0.5–2 mm) is light white and allotriomorphic.

## METHODS

After sampling, the material was crushed and then subjected to gravitational force and magnetic separation. The zircons were selected under a binocular lens, and then the particles and several reference samples (TEM) were placed on an epoxy resin target. They were then ground and used for transmission, reflection, cathode luminescence (CL) imaging, and SHRIMP U-Pb measurements. The CL images were taken at Institute of Geology, Chinese Academy of Geological Sciences.

The zircon U-Pb age data were generated from the SHRIMP II instrument of the Beijing SHRIMP Center (Institute of Geology, Chinese Academy of Geological Sciences). For detailed analytical procedures and principles, refer to Compston et al. (1992). The programs Ludwig SQUID 1.0 and ISOPLOT were used for data processing. A value recommended by the International Union of Geological Sciences (1977) was used as the age calculation constant. The error of a single data point is  $1\sigma$  and the weighted average age has a confidence level of 95%.

## RESULTS

A total of 18 measuring points for 18 zircons in Sample 1725 were subjected to SHRIMP U-Pb dating. The results are shown in

**TABLE 1** | SHRIMP Zircon U-Pb data of the granite dyke (Sample 1725) related to Dongxicun Kaolin deposit.

Spot	$^{206}\text{Pb}_c(\%)$	U (ppm)	Th (ppm)	$^{232}\text{Th}/^{238}\text{U}$	$^{206}\text{Pb}^*$ (ppm)	$^{207}\text{Pb}^*/^{206}\text{Pb}^*$	$\pm\%$	$^{207}\text{Pb}^*/^{235}\text{U}$	$\pm\%$	$^{206}\text{Pb}^*/^{238}\text{U}$	$\pm\%$	$^{206}\text{Pb}/^{238}\text{U}$ $\pm 1\sigma$ age (Ma)	$^{206}\text{Pb}/^{232}\text{Th}$ $\pm 1\sigma$ age (Ma)
1	--	374	91	0.25	45.7	0.0683	1.8	1.343	2.3	0.1426	1.4	859 $\pm 12$	901 $\pm 38$
2	--	300	38	0.13	35.8	0.0660	1.6	1.264	2.2	0.1390	1.5	839 $\pm 12$	893 $\pm 38$
3	--	382	64	0.17	47.8	0.06801	1.4	1.370	2.0	0.1461	1.5	879 $\pm 12$	926 $\pm 30$
4	1.68	1,193	132	0.11	155	0.0578	3.0	1.188	3.3	0.1490	1.4	895 $\pm 12$	628 $\pm 130$
5	0.14	589	51	0.09	74.8	0.0659	1.5	1.340	2.1	0.1475	1.4	887 $\pm 12$	910 $\pm 73$
6	0.05	291	40	0.14	35.1	0.0666	1.7	1.288	2.3	0.1403	1.5	846 $\pm 12$	797 $\pm 45$
7	--	285	38	0.14	34.4	0.0720	2.2	1.398	2.7	0.1407	1.5	849 $\pm 12$	1,092 $\pm 72$
8	--	370	60	0.17	45.6	0.0671	1.6	1.330	2.3	0.1437	1.7	866 $\pm 14$	891 $\pm 38$
9	--	324	47	0.15	40.6	0.0677	1.9	1.365	2.4	0.1461	1.5	879 $\pm 12$	897 $\pm 55$
10	--	420	62	0.15	56.8	0.06888	1.4	1.499	2.0	0.1578	1.4	945 $\pm 13$	1,018 $\pm 40$
11	0.45	439	54	0.13	64.5	0.0743	2.1	1.744	2.6	0.1702	1.4	1,013 $\pm 14$	683 $\pm 85$
12	0.55	296	51	0.18	40.5	0.0630	2.5	1.377	2.9	0.1586	1.5	949 $\pm 13$	716 $\pm 65$
13	0.04	665	127	0.20	79.6	0.06917	1.1	1.327	1.8	0.1392	1.4	840 $\pm 11$	675 $\pm 17$
14	1.16	891	221	0.26	112	0.0691	2.2	1.377	2.6	0.1445	1.4	870 $\pm 11$	1,059 $\pm 49$
15	0.87	701	121	0.18	92.4	0.0623	2.4	1.305	2.8	0.1521	1.4	913 $\pm 12$	834 $\pm 66$
16	0.07	326	52	0.16	39.1	0.0657	1.5	1.266	2.1	0.1398	1.5	844 $\pm 12$	852 $\pm 33$
17	--	405	196	0.50	51.3	0.0692	2.1	1.413	2.5	0.1482	1.4	891 $\pm 12$	907 $\pm 24$
18	--	215	262	1.26	28.7	0.0727	2.7	1.562	3.1	0.1559	1.6	934 $\pm 14$	928 $\pm 21$

Note:  $\text{Pb}_c$  and  $\text{Pb}^*$  represent common lead and radioactive lead, respectively. The measured  $^{204}\text{Pb}$  is used to correct the common lead in zircons, and the age is  $^{206}\text{Pb}/^{238}\text{U}$ .

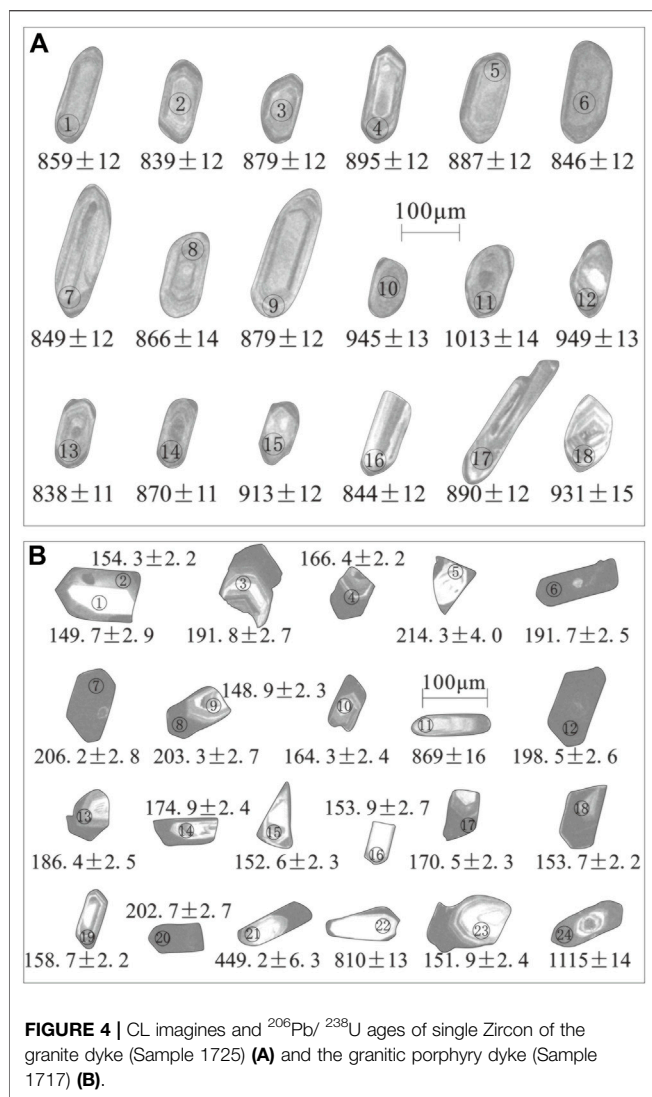
**Table 1** and the corresponding CL images are shown in **Figure 4A**. In Sample 1717, a total of 24 measuring points for 22 zircons were subjected to SHRIMP U-Pb dating, with the results shown in **Table 2** and corresponding CL images in **Figure 4B**.

The points 1725-4, 1725-5 and 1725-10 do not lie on the harmonic curves, with an age range of  $887 \pm 12$  Ma to  $945 \pm 13$  Ma. The measuring points can be divided into two groups distributed on the U-Pb harmonic curves (**Figures 5A,B**), except for 1725-11, 1725-12, 1725-15, 1725-17, and 1725-18 because they are relatively old ( $891 \pm 12$ – $1,013 \pm 14$  Ma). For the group with younger ages, the  $^{206}\text{Pb}/^{238}\text{U}$  age was weighted and averaged; an age of  $843 \pm 10$  Ma was obtained (MSWD = 0.12,  $n = 5$ ). The zircons are shaped like short columns and mostly have a ring structure, U contents of 285–665 ppm, and Th/U ratios of 0.13–0.20. They are magmatic zircons and represent the emplacement of the granite veins. The second group was characterized by relatively older  $^{206}\text{Pb}/^{238}\text{U}$  ages ( $871 \pm 11$  Ma, MSWD = 0.51,  $n = 5$ ), high U contents (324–889 ppm), and Th/U ratios of 0.15–0.26. The zircons are shaped like short to long columns and mostly have a ring structure; they could represent a record of the Jiuling tonalite wall rocks. The oldest zircons ( $891 \pm 12$  to  $1,013 \pm 14$  Ma) are mostly ellipsoidal, except for 1725-17 that is shaped like long columns, and most have a ring structure. They may represent a record of the regional wall rocks from the magma source area or the magma influx area.

The measuring points from Sample 1717 can be divided into two groups and distributed on the U-Pb harmonic curves (**Figures 5C,D**), except for 1717-11, 1717-21, 1717-22, and 1717-24, which are relatively older. In the first group, the  $^{206}\text{Pb}/^{238}\text{U}$  age was weighted and averaged and an age of  $152.3 \pm 1.8$  Ma (MSWD = 0.77,  $n = 7$ ) was obtained. The zircons are shaped like short columns (larger than the captured zircon particles) and most of them have a ring structure, U contents of 207–4,230 ppm, and Th/U ratios of 0.25–0.86. They are magmatic zircons and represent the

emplacement of granite porphyry veins. The second group has an  $^{206}\text{Pb}/^{238}\text{U}$  age of 170.5–206.2 Ma, high U contents (1957–26,130 ppm), and Th/U ratios of 0.05–0.28 (except for 1717-5). The zircons are shaped like short columns and most of them have no annulus structure. They may represent a record of the magma source area or unclosed U-Pb isotopic system. Zircons aged 869–810 Ma (1717-11 and 1717-22) are mostly shaped like long columns with no annulus structure, U contents of 118–359 ppm, and Th/U ratios of 0.1–0.46; these may represent a record of the Anlelin Formation wall rocks and/or Jiuling rocks. The zircons aged  $1,115 \pm 14$  Ma (1717-24) are shaped like long columns with a core-mantle structure, U contents of 1780 ppm, and Th/U ratio of 0.01, and may represent a basement record. The zircons aged  $449.2 \pm 6.3$  Ma (1717-21) are shaped like long columns with a core-mantle structure, U content of 782 ppm, and Th/U ratio of 0.26; these may represent a Caledonian thermal event.

The older zircon ages (891–1,013 Ma) captured in Sample 1725 are equivalent to the  $^{40}\text{Ar}/^{39}\text{Ar}$  age ( $928 \pm 19$  Ma) of the Xiwan albite granite in Dexing, Jiangxi ( $928 \pm 19$  Ma) (Hu et al., 1998) or the zircon U-Pb age of amphibole granite mixed into ophiolite (about 968 Ma) (Li et al., 1994), which may reflect residual rock fragments of the South China Sea (Yang et al., 2012; Wu et al., 2016) or the convergence, formation, and disintegration of the Rodinia Supercontinent (Hao and Zhai, 2004; Lu et al., 2004; Pan et al., 2016). The age of another group of zircons captured by granite veins is  $871 \pm 11$  Ma, which may be a record of the Jiuling tonalite wall rocks. This is slightly older than the SHRIMP zircon U-Pb age ( $855 \pm 5$  Ma) of the Cangxi schist tuff of Liuyang in the northeastern Hunan Province (Gao et al., 2011). The emplacement of the granite veins was dated to  $843 \pm 10$  Ma, which is older than ages of the northern margin of the Jiuling rock masses (837–816 Ma) (Zhong et al., 2005; Yuan et al., 2012; Sun et al., 2017; Duan et al., 2019; Wu et al., 2019) and the Shuangqiaoshan Group on the northern margin of Jiuling (840–819 Ma) (Gao et al., 2011; Zhou et al., 2012). This could



suggest that the formation of the Neoproterozoic tonalite masses on the Jiuling southern margin and the Anlelin Formation was slightly earlier than the rock masses and strata on the northern margin. Duan et al. (2017) showed that during extension, after the collision of the Neoproterozoic Cathaysian and Yangtze plates, magma on the southeastern Jiuling rock masses in the QHMB had a deep origin and early formation age, and that it gradually migrated toward the northwestern Jiuling rock masses.

The oldest zircon age of Sample 1717 is  $1,115 \pm 14$  Ma and may represent a basement record. It is consistent with the zircon U-Pb age for the volcanic rocks in the Tieshajie Formation complex ( $1,119 \pm 6$  Ma) (Cheng et al., 1991). Another group of older zircons captured by granite porphyry veins reflected ages of 869 to 810 Ma, which may be a record of the Anlelin Formation wall rocks and/or Jiuling rock masses. The age captured by the granite porphyry veins ( $449.2 \pm 6.3$  Ma) is a record of a Caledonian thermal event and is slightly older than the granites intruded into the Xinyu Iron Ore Area in the northern part of the QHMB ( $\sim 420$  Ma) (Zhang et al., 2018),

but is similar to the formation age of the early Caledonian granites in the eastern part of South China ( $440\text{--}460$  Ma) (Zhang F. R. et al., 2009) and the Wugongshan gneissic granite in Jiangxi ( $456.9 \pm 2.6$  Ma) (Lou et al., 2005). This suggests that at least one important tectonic magmatism event occurred in the late Early Paleozoic, which would be consistent with a lack of Lower Paleozoic strata in the Yichun area. The youngest age ( $152.3 \pm 1.8$  Ma, granite porphyry veins) represents the emplacement of the veins that become Kaolin deposits through weathered residualization. This is consistent with ages of the tungsten-tin-formation granites in southern Jiangxi ( $150\text{--}155$  Ma), such as the Zhangqiantang (Feng et al., 2007a), Hongtaoling (Feng et al., 2007b), Piaotang (Zhang et al., 2009b), and Tianmenshan (Liu et al., 2007) rock masses. This similarity indicates that during the period of tungsten-tin mineralization caused by large-scale magmatic activity in the southern Jiangxi (Nanling area), medium acid veins mostly intruded along fault structures on the southern margin of the Jiuling rock masses and became, upon weathering, Kaolin deposits rather than tungsten-tin deposits, which reflects differences in tectonic structure or magma source. The tungsten-tin mineralization is located on the Cathaysia Plate and the Kaolin deposits in the QHSZ between the Cathaysia and Yangtze plates. Emplacement ( $152.3 \pm 1.8$  Ma) of the Yinbeidong ore-forming granite porphyry veins (Sample 1717) was earlier than the metallogenic age (about 124 Ma) (Li et al., 2017) of the Gaoling Kaolin ore field in the Ehu rock base of northeastern Jiangxi (Zhao et al., 2010). The Yinbeidong Kaolin deposit is located in the Leping-Shexian mélangé sub-belt of the QHSZ and the Ehu Kaolin deposit in the Leping tectonic unit of the Yangtze Plate, suggesting that the acidic veins that form Kaolin deposits in the northern Jiangxi tend to migrate from south to north. Zircons captured by the granite porphyry veins were dated to  $170.5\text{--}206.2$  Ma and may represent the age record of the magma source area, be caused by an unclosed zircon U-Pb isotopic system, or high U contents ( $1957\text{--}26,130$  ppm). This can be seen in 1717-8 to 9, which are different parts of the same zircon. The age of the center with annulus structure is  $148.9 \pm 2.3$  Ma and the edge with no annulus structure is  $202.3 \pm 2.7$  Ma.

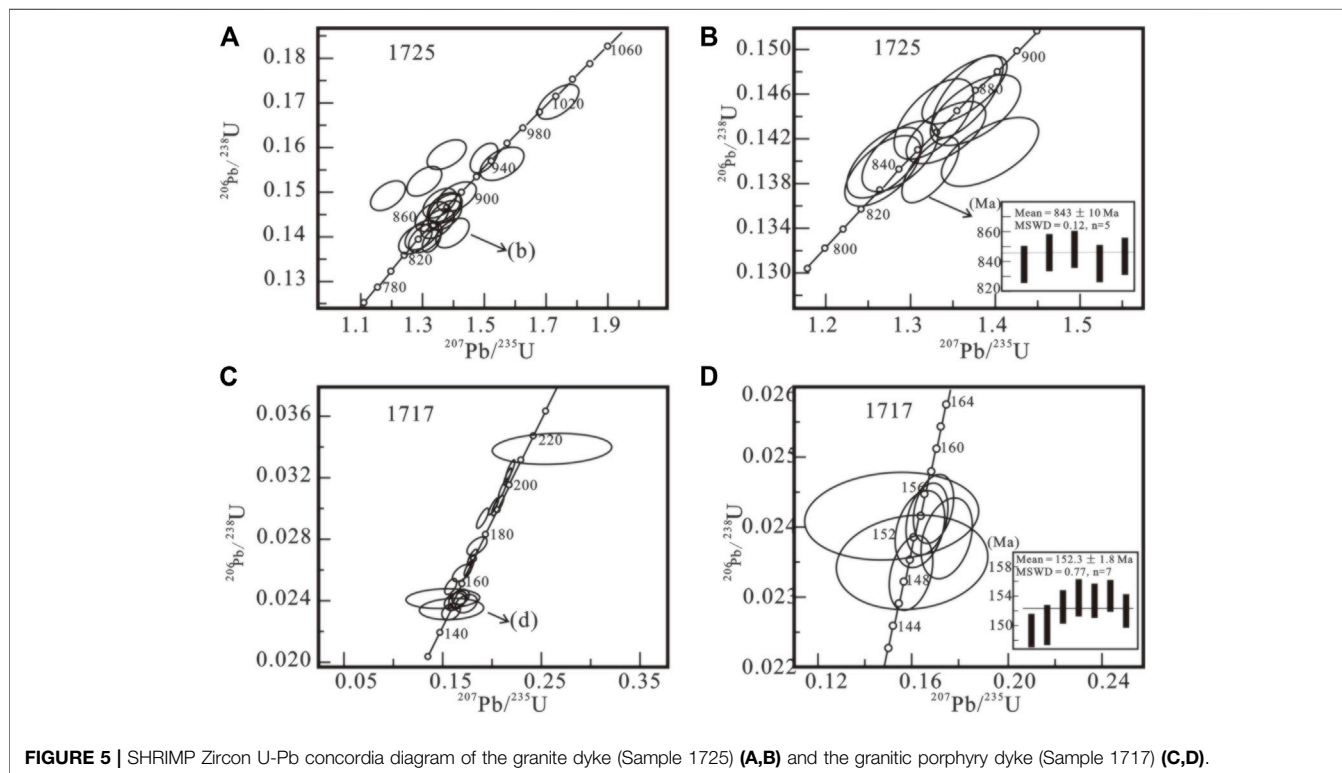
## DISCUSSION

The early Neoproterozoic thermo-tectonic event of the QHMB was the product of orogeny and the result of the convergence of the Rodinia Supercontinent (Lu et al., 2004) during the transition from Rodinia to the Gondwana Supercontinent (Zhou et al., 2008). This is slightly later than the typical Neoproterozoic Grenville orogen globally (Wang et al., 2017). Zhang (2013) proposed that the Neoproterozoic orogenic event in the Jiangnan Orogenic Belt is characterized by multi-period accretion and collage, and that evolution stages occur at: 1)  $\sim 880$  Ma, when the Shuangxiwu arc collaged to Cathaysia Plate; 2)  $860\text{--}838$  Ma, when the Jiangnan area was part of an arc-back-arc basin, with developed arc magmatism; 3)  $835\text{--}825$  Ma, when the Jiangnan

**TABLE 2** | SHRIMP Zircon U-Pb data of the granitic porphyry dyke (Sample 1717) related to Yinbeidong Kaolin deposit.

Spot	$^{206}\text{Pb}_c(\%)$	U (ppm)	Th (ppm)	$^{232}\text{Th}/^{238}\text{U}$	$^{206}\text{Pb}^*$ (ppm)	$^{207}\text{Pb}^*/^{206}\text{Pb}^*$	$\pm\%$	$^{207}\text{Pb}^*/^{235}\text{U}$	$\pm\%$	$^{206}\text{Pb}^*/^{238}\text{U}$	$\pm\%$	$^{206}\text{Pb}/^{238}\text{U} \pm 1\sigma$ age (Ma)	$^{206}\text{Pb}/^{232}\text{Th} \pm 1\sigma$ age (Ma)
1	0.20	207	133	0.67	4.19	0.0495	13	0.160	13	0.02350	1.9	149.7 $\pm$ 2.9	151 $\pm$ 13
2	--	1,210	292	0.25	25.2	0.0511	2.6	0.1706	3.0	0.02422	1.5	154.3 $\pm$ 2.2	155.9 $\pm$ 6.2
3	--	5,500	1,515	0.28	143	0.04959	1.3	0.2066	1.9	0.03021	1.4	191.8 $\pm$ 2.7	160.6 $\pm$ 3.4
4	0.02	4,230	2,366	0.58	95.1	0.04923	1.2	0.1775	1.8	0.02616	1.4	166.4 $\pm$ 2.2	160.6 $\pm$ 2.6
5	0.98	303	204	0.70	8.90	0.0561	15	0.262	16	0.03381	1.9	214.3 $\pm$ 4.0	203 $\pm$ 22
6	--	20,397	1,020	0.05	529	0.04876	0.51	0.2029	1.4	0.03019	1.3	191.7 $\pm$ 2.5	189.5 $\pm$ 4.5
7	0.00	21,091	1,001	0.05	589	0.04895	0.44	0.2194	1.4	0.03251	1.4	206.2 $\pm$ 2.8	191.2 $\pm$ 4.0
8	0.08	17,005	862	0.05	468	0.04889	0.60	0.2159	1.5	0.03203	1.3	203.3 $\pm$ 2.7	175.2 $\pm$ 6.5
9	--	579	448	0.80	11.6	0.0497	3.6	0.1599	3.9	0.02336	1.5	148.9 $\pm$ 2.3	144.1 $\pm$ 4.0
10	0.27	807	345	0.44	17.9	0.0479	3.3	0.1706	3.6	0.02581	1.5	164.3 $\pm$ 2.4	139.7 $\pm$ 4.9
11	0.93	359	34	0.10	44.9	0.0584	4.6	1.162	5.0	0.1443	2.0	869 $\pm$ 16	459 $\pm$ 190
12	--	26,130	1,387	0.05	702	0.04907	0.44	0.2116	1.4	0.03127	1.3	198.5 $\pm$ 2.6	198.6 $\pm$ 4.7
13	0.29	5,013	542	0.11	127	0.04742	1.6	0.1918	2.1	0.02933	1.4	186.4 $\pm$ 2.5	132.2 $\pm$ 8.9
14	0.45	1957	536	0.28	46.4	0.0489	3.3	0.1855	3.6	0.02750	1.4	174.9 $\pm$ 2.4	153.1 $\pm$ 8.1
15	--	593	342	0.60	12.2	0.0497	4.3	0.1643	4.5	0.02396	1.5	152.6 $\pm$ 2.3	148.7 $\pm$ 5.2
16	0.37	581	163	0.29	12.1	0.0454	16	0.151	16	0.02416	1.8	153.9 $\pm$ 2.7	146 $\pm$ 32
17	0.04	8,079	833	0.11	186	0.04889	1.1	0.1807	1.7	0.02681	1.4	170.5 $\pm$ 2.3	161.2 $\pm$ 5.6
18	--	1,187	413	0.36	24.6	0.0502	3.1	0.1670	3.4	0.02413	1.4	153.7 $\pm$ 2.2	157.5 $\pm$ 6.6
19	0.30	1,694	1,403	0.86	36.4	0.0465	2.2	0.1599	2.6	0.02493	1.4	158.7 $\pm$ 2.2	147.1 $\pm$ 2.9
20	0.03	23,396	1,250	0.06	642	0.04880	0.45	0.2149	1.4	0.03195	1.3	202.7 $\pm$ 2.7	177.4 $\pm$ 4.2
21	0.92	782	194	0.26	48.9	0.0586	4.2	0.583	4.5	0.0722	1.4	449.2 $\pm$ 6.3	273 $\pm$ 36
22	--	118	52	0.46	13.5	0.0693	6.6	1.280	6.8	0.1339	1.8	810 $\pm$ 13	864 $\pm$ 72
23	--	316	243	0.79	6.45	0.0533	3.8	0.1753	4.2	0.02384	1.6	151.9 $\pm$ 2.4	150.2 $\pm$ 4.6
24	0.42	1780	75	0.04	290	0.07869	0.92	2.049	1.6	0.1889	1.4	1,115 $\pm$ 14	

Note:  $\text{Pb}_c$  and  $\text{Pb}^*$  represent common lead and radioactive lead, respectively. The measured  $^{204}\text{Pb}$  is used to correct the common lead in zircons, and the age is  $^{206}\text{Pb}/^{238}\text{U}$ .

**FIGURE 5** | SHRIMP Zircon U-Pb concordia diagram of the granite dyke (Sample 1725) (A,B) and the granitic porphyry dyke (Sample 1717) (C,D).

area was in the co-collision–post-collision stage; 4) < 810 Ma, when the Jiangnan region entered the premature rift evolution environment.

The Neoproterozoic lithium deposits in South China are mostly produced in orogenic belts, and most ore bodies occur in late rock strans and altered granite and pegmatite veins of

compound rock masses (Shu et al., 2021). The Neoproterozoic massive sulfide polymetallic deposits in the QHMB are related to continental margin island arc volcanism. Neoproterozoic metamorphic Fe-Mn deposits are related to continental rifting volcanism and have experienced late transformation of regional metamorphism and thermal metamorphism (Xu et al., 2015).

In South China during the Mesozoic, the Tethyan Tectonic Domain was transformed into the Pacific Tectonic Domain because of the oblique subduction of the Izanagi Plate (Xie et al., 2005; Xu and Xie, 2005; Mao et al., 2008). Since the Jurassic, the Izanagi Plate has migrated to the NW and subducted under the Okhotsk Plate (Wan and Zhu, 2002). Wang and Shen (2003) suggested that early Mesozoic granite distributed east to west on the southern ridge of Jiangxi may be post-orogenic granite related to Indosinian movement. Together with associated bimodal volcanic rocks and A-type granite, they formed an extensional tectonic environment and homologous granitic intrusion–volcanic complex of South China in the late Mesozoic may be directly associated with the subduction of the Paleo-Pacific Plate under the Eurasian Plate. Li et al. (1999), Hu et al. (2004), and Peng et al. (2008) postulated that Mesozoic magmatic activity in South China was closed and correlated with lithospheric extension; low  $tMD$  and high  $\epsilon Nd$  belts are considered evidence for lithospheric extension and strong crust–mantle interactions (Hong et al., 2002). Previous studies investigated the relationship between Cretaceous granite magmatism and lithospheric extension in South China, and proposed five stages of granite emplacement events at 164–87 Ma (Li, 1999) or 180–80 Ma (Xie et al., 2005).

Mao et al. (2007) indicated that the large-scale tungsten–tin polymetallic mineralization in the middle and late Jurassic in the Nanling area is related to the subduction of the Paleo-Pacific Plate, with mineralization mostly occurring in the back-arc tectonic setting of the continental margin. Peng et al. (2008) indicated that the large-scale granite intrusion and explosive mineralization of tungsten, tin, and other metals in the middle section of Nanling were formed in a tectonic setting of lithospheric extension, thinning, and crustal extension that could be associated with the second Mesozoic lithospheric extension event in South China. Pei et al. (2008) demonstrated that the early tungsten–tin mineralization of Nanling strata in the Mesozoic was associated with deep tectonic–magmatic processes, crustal magma–tectonic power, and an intrusive contact tectonic system formed during the tectonic–magmatism of continental margin–intracontinental orogeny. Hua (2005) proposed that the mineralization of tungsten and tin was related to dynamic extension background, crust–mantle interactions, and the participation of deep heat fluids. Li et al. (2008) indicated that the middle–late Jurassic tungsten mineralization and multi-stage tungsten–tin mineralization in South China were the result of multi-stage subduction of oceanic plates (or ridges) during different periods. Lin et al. (2020) estimated the difference in basement depth between the QHSZ and the Cathaysian Plate through seismic sounding and calculated depths of 0.5–2.0 km (QHSZ) and 1.5–3.0 km (Cathaysian Plate), with the QHSZ extending at least 8 km deep. This led to the hypothesis that

differences in basement depth, fault properties, and deep magmatism cause differences in mineralization.

## CONCLUSION

The SHRIMP U-Pb dating of zircons in ore-forming veins of weathered residual Kaolin deposits on the northern QHMB margin showed that the ore-forming granite veins intruding into the Jiuling rock masses are Neoproterozoic ( $843 \pm 10$  Ma) in age and the ore-forming granite porphyry veins intruding into Neoproterozoic Anlelin Formation strata are late Jurassic ( $152.3 \pm 1.8$  Ma). We suggest that there were two periods in the formation of ore-forming rock masses of Kaolin deposits on the northern QHMB margin. Neoproterozoic Kaolin-forming veins may be related to the convergence, formation, or disintegration of the Rodinia Supercontinent and the Jurassic Kaolin-forming veins may be related to the subduction of the Paleo-Pacific Plate. Therefore, subsequent investigations and evaluations of weathered residual Kaolin deposits on the QHMB need to strengthen the identification and evaluation of late Jurassic and, particularly, Neoproterozoic acidic veins.

## DATA AVAILABILITY STATEMENT

The original contributions presented in the study are included in the article/Supplementary Material, further inquiries can be directed to the corresponding author.

## AUTHOR CONTRIBUTIONS

CL wrote the initial draft of the work and the final paper. CL, XZ and WZ interpreted the experiments and scanning electron microscope images. CL, QS, ZS, RC and TG contributed in interpreting the results. All authors finally approve the manuscript and thus agree to be accountable for this work.

## FUNDING

This research was financially supported by China Geological Survey (DD20211579, DD20160038) and the NSF of China (41102052).

## ACKNOWLEDGMENTS

We acknowledge Liu Shoujie (National Science and Technology Infrastructure Platform Beijing SHRIMP Center) for his assistance in sample loading, instrument commissioning and monitoring, and data processing. We also thank Li Qiming from China University of Geosciences (Wuhan), Yang Haoran and Liu Meng from Chengdu University of Technology, and Xie Rongbo, from China University of Petroleum (Beijing) for their help in the field and with sample collection. Finally, we thank Sev Kender, PhD, from Liwen Bianji (Edanz) ([www.liwenbianji.cn/](http://www.liwenbianji.cn/)), for editing the English text of a draft of this manuscript.

## REFERENCES

- Cheng, H., Hu, S. L., and Tang, Z. H. (1991). New Recognition on the Isotopic Geochronology of the "Tieshajie Group" in the Southern Part of Northeastern Jiangxi. *Reg. Geology China* 2, 151–154.
- Compston, W., Williams, I. S., Kirschvink, J. L., Zichao, Z., and Juogan, M. A. (1992). Zircon U-Pb Ages for the Early Cambrian Time-Scale. *J. Geol. Soc.* 149, 171–184. doi:10.1144/gsjgs.149.2.0171
- Duan, Z., Liao, S. B., Chu, P. L., Huang, W. C., Zhu, Y. H., Shu, X. J., et al. (2019). Zircon U-Pb Ages of the Neoproterozoic Jiuling Complex Granitoid in the Eastern Segment of the Jiangnan Orogen and its Tectonic Significance. *Geology China* 3, 493–516. CNKI:SUN:DIZI.0.2019-03-006.
- Feng, C. Y., Feng, Y. D., Xu, J. X., Zeng, Z. L., She, H. Q., Zhang, D. Q., et al. (2007a). Isotope Chronological Evidence for Upper Jurassic Petrogenesis and Mineralization of Altered Granite-type Tungsten Deposits in the Zhangtiantang Area, Southern Jiangxi. *Geology China* 4, 642–650. doi:10.3969/j.issn.1000-3657.2007.04.013
- Feng, C. Y., Xu, J. X., Zeng, Z. L., Zhang, D. Q., Qu, W. J., She, H. Q., et al. (2007b). Zircon SHRIMP U-Pb and Molybdenite Re-os Dating in Tianmenshan-Hongtaoling Tungsten-Tin orefield, Southern Jiangxi Province, China, and its Geological Implication. *Acta Geologica Sinica* 7, 952–963. doi:10.3321/j.issn:0001-5717.2007.07.011
- Gao, L. Z., Chen, J., Ding, X. Z., LiuZhang, Y. R. C. H., Zhang, H., Liu, Y. X., et al. (2011). Zircon SHRIMP U-Pb Dating of the Tuff Bed of Lengjiaxi and Banxi Groups, Northeastern Hunan, Constraints on the Wuling Movement. *Geol. Bull. China* 7, 1001–1008. 1671-255207-1001-0.
- Hao, J., and Zhai, M. G. (2004). Jinning Movement and Sinian System in China, Their Relationship with Rodinia Supercontinent. *Chin. J. Geology* 1, 139–152. doi:10.3321/j.issn:0563-5020.2004.01.014
- Hong, D. W., Xie, X. L., and Zhang, J. S. (2002). Geological Significance of the Hangzhou-Zhuguangshan-Huashan High- $\epsilon$ Nd Granite belt. *Geol. Bull. China* 6, 348–354. doi:10.3969/j.issn.1671-2552.2002.06.012
- Hu, S. L., Hao, J., and Li, Y. J. (1998).  $^{40}\text{Ar}/^{39}\text{Ar}$  Isochron Age of the Xiwan Albite Granite in Dexing, Jiangxi, Determined by the Laser Mass Spectrometry. *Reg. Geology China* 1, 66–68. doi:10.1088/0256-307X/15/11/025
- Hua, R. M. (2005). Differences between Rock-Forming and Related Ore-Forming Times for the Mesozoic Granitoids of Crust Remelting Types in the Nanling Range, South China, and its Geological Significance. *Geol. Rev.* 6, 633–639. CNKI:SUN:DZLP.0.2005-06-005.
- Jiang, S. Y., Peng, N. J., Huang, L. C., Xu, Y. M., Zhan, G. L., and Dan, X. H. (2015). Geological Characteristic and Ore Genesis of the Giant Tungsten Deposits from the Dahutang Ore-Concentrated District in Northern Jiangxi Province. *Acta Petrologica Sinica* 3, 639–655. CNKI:SUN:YSXB.0.2015-03-001.
- Li, N., Wu, X. L., Wu, D. X., Zhou, C., and Hu, F. L. (2017). Geological Features and Utilization prospect of Ehu Kaolin Deposit in Fuliang County, Jiangxi Province. *J. East China Univ. Technol. (Natural Sciences)* 2, 149–157. doi:10.3969/j.issn.1674-3504.2017.02.007
- Li, X. F., Watanabe, Y., Hua, R. M., and Mao, J. W. (2008). Mesozoic Cu-Mo-W-Sn Mineralization and ridge/Triple Subduction in South China. *Acta Geologica Sinica* 5, 625–640. doi:10.3321/j.issn:0001-5717.2008.05.006
- Li, X. H., Zhou, G. Q., and Zhao, X. J. (1994). SHRIMP Ion Microprobe Zircon U-Pb Age of the NE Jiangxi Ophiolite and its Tectonic Implications. *Geochimica* 2, 125–131. CNKI:SUN:DQHX.0.1994-02-002.
- Lin, J. Y., Tang, G. B., Xu, T., Cai, H. T., Lü, Q. T., Bai, Z. M., et al. (2020). P-wave Velocity Structure in Upper Crust and Crystalline Basement of the Qinhang and Wuyishan Metallogenic Belts, Constraint from the Wanzai-Hui'an Deep Seismic Sounding Profile. *Chin. J. Geophys.* 12, 4396–4409. doi:10.6038/cjg202000158
- Liu, S. B., Wang, D. H., Chen, Y. C., Xu, J. X., Zeng, Z. L., Ying, L. J., et al. (2007). SHRIMP Dating of Tianmenshan Granite Pluton and Granite-Porphry Dyke in Southern Jiangxi Province, Eastern Nanling Region and its Significance. *Acta Geologica Sinica* 7, 972–978. doi:10.3321/j.issn:0001-5717.2007.07.013
- Lou, F. S., Shen, W. Z., Wang, D. Z., Shu, L. S., Wu, F. J., Zhang, F. R., et al. (2005). Zircon U-Pb Isotopic Chronology of the Wugongshan Dome Compound Granite in Jiangxi Province. *Acta Geologica Sinica* 5, 636–644. doi:10.3321/j.issn:0001-5717.2005.05.008
- Lu, S. N., Li, H. K., Chen, Z. H., Yu, H. F., Jin, W., and Guo, K. Y. (2004). Relationship between Neoproterozoic Cratons of China and the Rodinia. *Earth Sci. Front.* 2, 515–523. doi:10.3321/j.issn:1005-2321.2004.02.021
- Mao, J. W., Xie, G. Q., Guo, C. L., and Chen, Y. C. (2007). Large-scale Tungsten-Tin Mineralization in the Nanling Region, South China, Metallogenic Ages and Corresponding Geodynamic Processes. *Acta Petrologica Sinica* 10, 2329–2338. doi:10.3969/j.issn.1000-0569.2007.10.002
- Mao, J. W., Xie, G. Q., Guo, C. L., Yuan, S. D., Cheng, Y. B., and Chen, Y. C. (2008). Spatial-temporal Distribution of Mesozoic Ore Deposits in South China and Their Metallogenic Settings. *Geol. J. China Universities* 4, 510–526. doi:10.3969/j.issn.1006-7493.2008.04.005
- Pan, G. T., Lu, S. Ni., Xiao, Q. H., Zhang, K. X., Yin, F. G., Hao, G. J., et al. (2016). Division of Tectonic Stages and Tectonic Evolution in China. *Earth Sci. Front.* 6, 1–23. doi:10.13745/j.esf.2016.06.00
- Pei, R. F., Wang, Y. L., Li, L., and Wang, H. L. (2008). South China Great Granite Province and its Metallogenic Series of Tungsten-Tin Poly-Metallics. *China Tungsten Industry* 1, 10–13. doi:10.3969/j.issn.1009-0622.2008.01.003
- Peng, J. T., Hu, R. Z., Yuan, S. D., Bi, X. W., and Shen, N. P. (2008). The Time Ranges of Granitoid Emplacement and Related Nonferrous Metallic Mineralization in Southern Hunan. *Geol. Rev.* 5, 617–625. doi:10.3321/j.issn:0371-5736.2008.05.006
- Shu, L. S., Zhu, W. B., and Xu, Z. Q. (2021). Geological Settings and Metallogenic Conditions of the Granite-type Lithium Ore Deposits in South China. *Acta Geologica Sinica* 10, 3099–3114. doi:10.7762/j.cnki.dizhixuebao.2021152
- Sun, K. K., Chen, B., Chen, J. S., and Xiang, X. K. (2017). The Petrogenesis of the Jiuling Granodiorite from the Dahutang deposit, Jiangxi Province and its Tectonic Implications. *Acta Petrologica Sinica* 3, 907–924. doi:10.00-0569/2017/033(03)-0907-24
- Wan, T. F., and Zhu, H. (2002). 2. Tectonics and Environment Change of Mesozoic in China Continent and its Adjacent Areas. *Geoscience - J. Graduate Sch. Beijing: China University of Geosciences*, 107–120. doi:10.3969/j.issn.1000-8527.2002.02.001
- Wang, D. Z., and Shen, W. Z. (2003). Genesis of Granitoids and Crustal Evolution in Southeast China. *Earth Sci. Front.* 3, 209. doi:10.3321/j.issn:1005-2321.2003.03.020
- Wang, F. N., Zhou, Y. H., and Yu, C. F. (1986). Kaolin Deposits and Their Geological Characteristics in Jiangxi. *Geology China* 1, 18–20. CNKI:SUN:DIZI.0.1986-01-007.
- Wang, G. L., Hu, J. S., Hu, F. L., Zhao, L. M., and Hu, G. H. (2018). Characteristics and Prospecting Direction of Pulse Type Kaolin in Jingdezhen-A Case of Study in Ehu Kaolin deposit. *J. East China Univ. Technol. (Natural Sciences)* 4, 379–388. doi:10.3969/j.issn.1674-3504.2018.04.010
- Wang, X. L., Zhou, J. C., Chen, X., Zhang, F. F., and Sun, Z. M. (2017). Formation and Evolution of the Jiangnan Orogen Belt. *Bull. Mineralogy, Petrol. Geochem* 5, 714–735. doi:10.3969/j.issn.1007-2802.2017.05.003
- Wang, Y. J., and Fang, Y. S. (1994). Discussion on the Formation Mechanism of High Quality Kaolin Ore in Yichun, Jiangxi Province. *Nonmetallic Geology*. 6, 2–7.
- Wu, F. J., Yu, J., Liu, C. G., and Deng, J. H. (2016). Basic Features and Significance of Yifeng-Dexing Superimposition Orogenic belt, Jiangxi Province. *Geol. Bull. China* 1, 181–187. doi:10.3969/j.issn.1671-2552.2016.01.017
- Wu, X. Y., Zhang, Z. Y., Zheng, Y. C., Dai, J. L., Fan, X. K., and Sheng, Y. C. (2019). Magmatism, Genesis and Significance of Multi-Stage Porphyry-like Granite in the Giant Dahutang Tungsten deposit, Northern Jiangxi Province. *Acta Petrologica et Mineralogica* 3, 318–338. doi:10.3969/j.issn.1000-6524.2019.03.003
- Xie, G. Q., Mao, J. W., Hu, R. Z., Li, R. L., and Cao, J. J. (2005). Discussion on Some Problems of Mesozoic and Cenozoic Geodynamics of Southeast China. *Geol. Rev.* 6, 613–620. doi:10.3321/j.issn:0371-5736.2005.06.002
- Xu, D. M., Lin, Z. Y., Luo, X. Q., Zhang, K., Zhang, X. H., and Huang, H. (2015). Metallogenic Series of Major Metallic Deposits in the Qinzhou-Hangzhou Metallogenic belt. *Earth Sci. Front.* 2, 7–24. CNKI:SUN:DXQY.0.2015-02-003.
- Xu, X. S., and Xie, X. (2005). Late Mesozoic-Cenozoic Basaltic Rocks and Crust-Mantle Interaction, SE China. *Geol. J. China Universities* 3, 318–334. 006-749303-318-17.
- Yang, M. G., Liu, Y. G., Huang, Z. Z., Wu, F. J., and Song, Z. R. (2012). Subdivision of Meso-Neoproterozoic Strata in Jiangxi and a Correlation with the Neighboring Areas. *Geology China* 1, 43–54. CNKI:SUN:DIZI.0.2012-01-006.

- Yuan, Y., Liao, Z. T., and Wang, C. (2012). Multi-stage Tectonic Evolution in Jiangnan Uplift (Jiuling Terran) from Granitoids Records. *J. Tongji Univ. (Natural Sciences)* 9, 1414–1421. doi:10.3969/j.issn.0253-374x.2012.09.023
- Zhang, F. R., Shu, L. S., Wang, D. Z., Yu, J. H., and Shen, W. Z. (2009a). Discussions on the Tectonic Setting of Caledonian Granitoids in the Eastern Segment of South China. *Earth Sci. Front.* 1, 248–260. CNKI:SUN:DXQY.0.2009-01-034
- Zhang, J. L., Xu, D. R., Yu, L. L., and Hou, M. Z. (2018). Zircon U-Pb Dating of Granite and Host Rock in Xinyu Iron Ore Area, Jiangxi Province, China. *Chin. J. Nonferrous Met.* 5, 971–984. doi:10.19476/j.ysxb.1004.0609.2018.05.14
- Zhang, W. L., Hua, R. M., Wang, R. C., Li, H. M., Qu, W. J., and Ji, J. Q. (2009b). New Dating of the Piaotang Granite and Related Tungsten Mineralization in Southern Jiangxi. *Acta Geologica Sinica* 5, 659–670. doi:10.3321/j.issn:0001-5717.2009.05.007
- Zhao, P., Jiang, Y. H., Liao, S. Y., Zhou, Q., and Jin, G. D. (2010). SHRIMP Zircon U-Pb Age, Sr-Nd-Hf Isotopic Geochemistry and Petrogenesis of the Ehu Pluton in Northeastern Jiangxi Province. *Geol. J. China Universities* 2, 218–225. doi:10.3969/j.issn.1006-7493.2010.02.009
- Zhong, Y. F., Ma, C. Q., She, Z. B., Lin, G. C., Xu, H. J., Wang, R. J., et al. (2005). SHRIMP U-Pb Zircon Geochronology of the Jiuling Granitic Complex Batholith in Jiangxi Province. *Earth Sci.* 6, 685–691. doi:10.3321/j.issn:1000-2383.2005.06.005
- Zhou, J. C., Wang, X. L., and Qiu, J. S. (2008). Is the Jiangnan Orogenic Belt a Grenvillian Orogenic Belt, Some Problems about the Precambrian Geology of South China. *Geol. J. China Universities* 1, 64–73. CNKI:SUN:GXDX.0.2008-01-009.
- Zhou, X. H., Zhang, Y. J., Liao, S. B., Yu, M. G., Chen, Z. H., Zhao, X. L., et al. (2012). LA-ICP-MS Zircon U-Pb Geochronology of Volcanic Rocks in the Shuangqiaoshan Group at Anhui-Jiangxi Boundary Region and its Geological Implication. *Geol. J. China Universities* 4, 609–622. CNKI:SUN:GXDX.0.2012-04-005.

**Conflict of Interest:** The authors declare that the research was conducted in the absence of any commercial or financial relationships that could be construed as a potential conflict of interest.

**Publisher's Note:** All claims expressed in this article are solely those of the authors and do not necessarily represent those of their affiliated organizations, or those of the publisher, the editors, and the reviewers. Any product that may be evaluated in this article, or claim that may be made by its manufacturer, is not guaranteed or endorsed by the publisher.

Copyright © 2022 Li, Sun, Sun, Zhou, Zhang, Chen and Gao. This is an open-access article distributed under the terms of the Creative Commons Attribution License (CC BY). The use, distribution or reproduction in other forums is permitted, provided the original author(s) and the copyright owner(s) are credited and that the original publication in this journal is cited, in accordance with accepted academic practice. No use, distribution or reproduction is permitted which does not comply with these terms.